

Skin Melanoma Detection, Classification and Performance Measurement using Random Forest Classifier

Sheetal N. Patil *, Hitendra D. Patil **

* Research Scholar, Department of Computer Engineering, S.S.V.P.S College of Engineering Dhule-424005

** Professor, Department of Computer Engineering S.S.V.P.S College of Engineering Dhule-424005

ABSTRACT

The fourth greatest source of non-fatal diseases affecting 30-70% of the population worldwide is skin disease, and it is common across geography and ages. Skin disease is the predominant form of skin cancer in the United States. Skin disease is one of the most common health problems. In order to provide statistical representations on suspended areas, computer-operated diagnostic systems require sophisticated image processing algorithms. In this article we analyzed the latest scientific progress used for the diagnostic methods for computer-aided skin lesions. The phases include pre-processing of skin lesions, segmentation, collection of features and the recognition of particular characteristics.

In this paper we implemented Random Forest (RF) classification algorithm to classify benign and malignant small skin image dataset. In RF classifier Bootstrap aggregation and selection of K and N node is key stage which decide performance of algorithm. Classifier Performance was improved in terms of accuracy (+3.44%), Area under ROC (+1.05%), precision (-0.8%) during cross validation score. Results show that RF classifier is able to achieve classification accuracy 86.90% for malignant cases and similarly 88.67 % for benign cases.

Keywords - Accuracy, Aggregation, Benign, Malignant, Random Forest, Skin Melanoma

I. INTRODUCTION

Critical skin disorders include melanoma. The reports indicate that in fourth cases, the melanoma is found in benign form, and in other cases, malignant. Precise early-stage melanoma diagnosis may improve the patient survival rates significantly. Conversely, conventional methods of detection of melanoma require tremendous skin disease specialization, requiring inter-observer variations for each patient. There is definitely a requirement that an automated melanoma detection system be created, which will allow the pathologist to diagnose more accurately skin diseases. Skin is the largest aspect of the human body astronomically. The composition of the skin is complex and contains many layers. The three main characteristics of the skin are Auspice, Sensation and Thermoregulation: the subcutaneous layer, dermis and epidermis layers. Stratum corneum is the upper layer of a protective epidermis that is of various thicknesses optically neutral.

Melanocytes are found in the basal epidermis layer. The skin pigment, called melanin, is produced by melanocytes, which provide the bronze or brown skin. Depending on the melanocyte stage, the extent to which UV rays absorb. In the interior skin structure Fig.1 reflects the various layers. The epidermis is an ultimate skin layer, creating a waterproof protection and generating a tone of the skin. Skin has three stages. Dermal

tissue, hair follicles and sweat glands are found in the dermis below the epidermis. The deeper tissue of the subcutaneous system is fat and binding. Dermis consists of blood vessels, filters, antibodies, collagen fibers, and nerve ends, and is the middle layer of the skin. It gives the skin strength and elasticity.

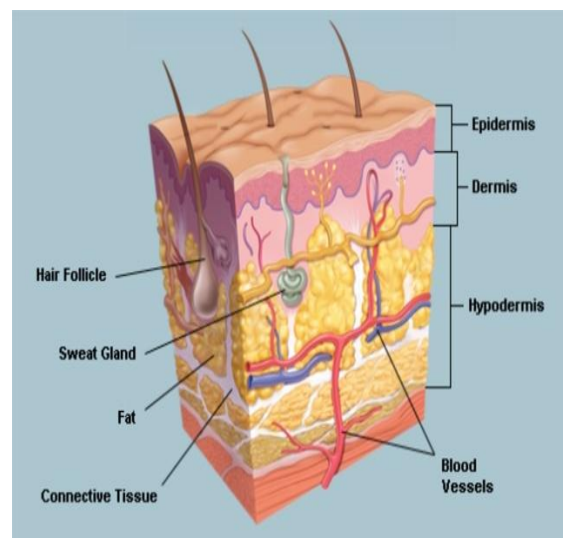


Fig.1-Skin Internal Structure with Different Layers

Skin cancer constituted (3.18%) 84 out of 2638 patients registered with cancer of all types. The age of the patients was 62 ± 14.2 years and

ranged from 27 to 92 yrs. Basal cell carcinoma (BCC) was the most common histological type (46/84, 54.76%) followed by Squamous cell carcinoma (SCC) (31/84, 36.91%) and malignant melanoma (MM) (7/84, 8.33%). Male: female ratio was found to be 0.79:1. BCC showed higher female preponderance ($p < 0.05$). Head and Neck was the commonest site involved ($p < 0.05$). Majority (88%) of patients were from rural area. 92% of patients were directly into the profession of agriculture with history of prolonged exposure to sunlight. An estimated 196,060 cases of melanoma will be diagnosed in the U.S. in 2020. Of those, 95,710 cases will be in situ (noninvasive), confined to the epidermis (the top layer of skin), and 100,350 cases will be invasive, penetrating the epidermis into the skin's second layer (the dermis). Of the invasive cases, 60,190 will be men and 40,160 will be women.

II. MELANOMA TYPES & SKIN LESION DETECTION METHOD.

Preprocessing methods improve image quality by reducing artefacts. Displays the evaluation vectors that concentrate the segmentation of the picture with the extraction and choice of the function. Segmented pixels divided into zones and thus tissue boundaries were created. Segmentation accompanied by grouping or marking of regions into tissue types. Precise dermoscopic image segmentation has become essential in accordance to the tissue type. Diagnosis, treatment preparation is efficacious in skin cancer studies. Changes to the composition of the skin tissue may be used for identifying, understanding and broadly explaining physiological processes. The overall flow of automated system consists of following steps as illustrate in fig 2.

The extraction of features is a technique used to evaluate the important features in an image that are useful for the application. Early melanoma form detection is distinguished by colour, skin lesions texture, and geometric characteristics. Various researches on the extraction of characteristics of segmented areas were conducted. Segmentation refers to a division into separate regions of the dermoscopic image containing the same properties of all pixels. The performance of medical image analysis depends on the accuracy of segmentation and it is generally very difficult to precisely

Segment the image. Manual boundary detection protects the root problem due to overlap of the tumor. Accurate segmentation therefore requires greater awareness of the lesion characteristics. In comparison, boundary errors will impact the classification process less.

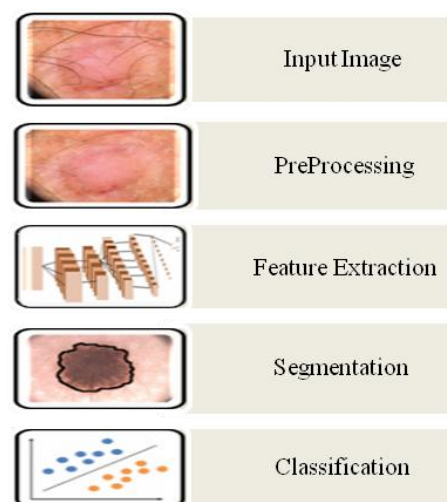


Fig.2- Skin Lesion Detection & Processing

The dermoscopic images can be classified into nine different diagnostic categories depicted as below

- Melanoma
- Basal cell carcinoma
- Actinic keratosis
- Vascular lesion
- Squamous cell carcinoma
- Benign keratosis
- Melanocytic nevus
- Dermatofibroma
- None of the others

There are currently extremely exciting possibilities for an early screening system which concentrates on computer-based evaluation of dermoscopic images. Segmentation is an automated development method for creating an efficient computerized skin lesion analysis system. This provides significant space for research to include a computer-based analytical system for dermoscopic images. Early detection is important to timely diagnosis and treatment preparation for early detection and segmentation of the skin lesions. Intra- and inter-observer dermatologist distinguishes make the device unsuitable during manual detection time. In the manual detection system, this problem leads to the implementation of a precise and automated system. We explored various techniques and approaches to detect and classify skin lesions to resolve this issue. In the development of an efficient system, machine learning characteristics play an important role. The general characteristics considered during previous research are colour, texture, form, asymmetry and borders. Specificity, precision, false prediction value and Matthews' correlation coefficient (MCC) are considered for calculating the performance of various classification algorithms.

III. RANDOM FOREST (RF) TECHNIQUE

A number of widely used dermatology ML algorithms are present. For example, a linear regression, logistic regression, k-nearest neighbor (k-NN), support of the vector machine (SVM), random woodland (RF) and natural language processing, some of the most common statistical learn tool, are the ML-algorithms (NLP). The k-NN shall be used as a basis of k neighbors for data classification and regression. SVMs were used to classify data by looking for an inter-group hyper plane. RFs create an arbitrary preference network to find the most common result of all altered decision trees RFs.

Random Forest is a common learning machine algorithm belonging to the methodology of supervised learning. It can be used both for the problems of classification and regression in ML. It is based on the principle of ensemble learning, a method by which several graders are merged to overcome a complex problem and boost model efficiency. Random Forest works in two-phase first is to create the random forest by combining N decision tree, and second is to make predictions for each tree created in the first phase. Following are some advantages which motivate to select algorithm Random Forest:

- Compared to other algorithms, it requires less preparation.
- It predicts high-precision performance, except for the large data set.
- It can also be precise if a significant part of the data is unavailable.

The Working process can be explained in the below steps

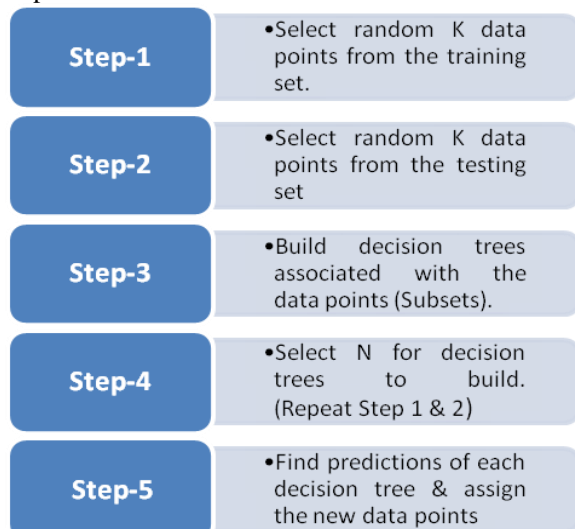


Fig.3- Working Process & Parameter Selection in RF Algorithm.

The training algorithm for random forests applies the general technique of bootstrap aggregating, or bagging, to tree learners.

Given a training set $X = x_1, x_2, \dots, x_n$ with responses $Y = y_1, y_2, \dots, y_n$ bagging repeatedly to selects a random sample with replacement of the training set and fits trees to these samples. After training, predictions for unseen samples x' can be made by averaging the predictions from all the individual regression trees on x' is calculated by equation (1)

$$f = \frac{1}{N} \sum_{n=0}^N f_b(x)^n \quad (1)$$

For each decision tree, Scikit-learn calculates a nodes importance using Gini Importance, assuming only two child nodes (binary tree) shown in equation (2)

$$n_j^i = \{w_j.cj - w_{left.cleft} - w_{right.cright}\}^n \quad (2)$$

Where,

- $n_{sub(j)}$ = the importance of node j
- $w_{sub(j)}$ = weighted no.of samples reaching node j
- $C_{sub(j)}$ = the impurity value of node j
- $left(j)$ = child node from left split on node j
- $right(j)$ = child node from right split on node j

The importance for each feature on a decision tree is then calculated by equation (3) and calculates weighted value for each node

$$f^{(i)} = \sum_j: \text{node } j \text{ splits on feature } i n_j^i \quad (3)$$

IV. PERFORMANCE PARAMETER & RESULTS

Random forests are considered as a highly accurate and robust method because of the number of decision trees participating in the process. It does not suffer from the over fitting problem. Fig 4 shows RF classifier performance in terms of false positive rate (FPR) & True Positive rate (TPR) for Binary Classification Problem if Cancer is BENIGN/MALIGNANT

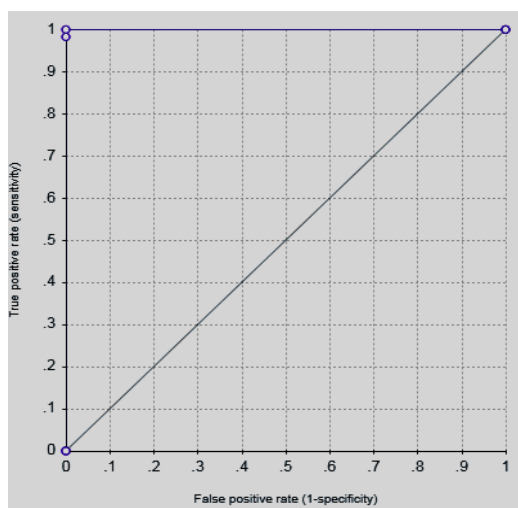


Fig.4- Correlation between FPR & TPR for RF.

Evaluation Parameter	Holdout Score
Accuracy	89.90%
Area under ROC curve	94.25%
Precision	96.80%
Recall	89.90%
F1 Measure	92.62%
Average Precision	93.45%
Log Loss	10.25%
Accuracy	89.90%

Table 1: Model Evaluation Holdout Score

Evaluation Parameter	Cross Validation Score
Accuracy	93.34%
Area under ROC curve	95.23%
Precision	96.00%
Recall	87.23%
F1 Measure	92.45%
Average Precision	97.23%
Log Loss	11.25%
Accuracy	93.34%

Table 2: Model Evaluation cross validation Score

RF classifier performance parameter was calculated in terms of accuracy, ROC, Precision, Recall and F1 shown in Table 1 for holdout score selection on IBN Watson. Similarly for cross validation score was calculated & represented in Table 2

Confusion Matrix:

In the confusion matrices below, the rows represent the true labels and the columns represent predicted labels. Values on the diagonal represent the number (or percent, in a normalized confusion matrix) of times where the predicted label matches the true label. For Benign& malignant confusion

matrix performance is shown in Table3.

Observed	Predicted	
	Malignant	Benign
Malignant	58.00%	0 %
Benign	0	3.255%
True Classification %	86.90%	88.67%

Table 3: Confusion Matrix for RF Classifier

V. CONCLUSION & FUTURE SCOPE

In this paper we implemented Random forest based skin image classification for benign and malignant cases; this approach is used to calculate classification performance parameter in terms of Accuracy, area under ROC, Average precision and many more.

From performance results it is observed that performance parameters increases during cross validation score as compared to Holdout score using IBM Watson. Random forest (RF) algorithm is effectively classifying malignant & benign skin image dataset with maximum 86.90 % & 88.67 % respectively. Linear correlation between false positive rate and True positive rate during classification direct us to improve many design parameters during training & testing. The random forest technique can also handle big data with numerous variables running into thousands. It can automatically balance data sets when a class is more infrequent than other classes in the data. The method also handles variables fast, making it suitable for complicated tasks.

REFERENCES

- [1]. F. Dalila, A. Zohra, K. Reda, and C. Hocine, "Segmentation and classification of melanoma and benign skin lesions," *Optik - International Journal for Light and Electron Optics*, vol. 140, pp. 749–761, 2017.
- [2]. M. E. Celebi, Y. A. Aslandogan, W. V. Stoecker, H. Iyatomi, H. Oka, and X. Chen, "Unsupervised border detection in dermoscopy images," *Skin Research and Technology*, vol. 13, no. 4, pp. 454–462, 2018.
- [3]. H. Fan, F. Xie, Y. Li, Z. Jiang, and J. Liu, "Automatic segmentation of dermoscopy images using saliency combined with Otsu threshold," *Computers in Biology and Medicine*, vol. 85, pp. 75–85, 2017.
- [4]. D. D. Gómez, C. Butakoff, B. K. Ersbøll, and W. Stoecker, "Independent histogram pursuit for segmentation of skin lesions," *IEEE Transactions on Biomedical Engineering*, vol. 55, no. 1, pp. 157–161, 2018.
- [5]. D. A. Okuboyejo, O. O. Olugbara, and S. A. Odunaike, "Unsupervised restoration of hair-

- occluded lesion in dermoscopic Images,” in *MIUA*, pp. 91–96, 2014.
- [6]. J. Premaladha and K. S. Ravichandran, “Novel Approaches for Diagnosing Melanoma Skin Lesions Through Supervised and Deep Learning Algorithms,” *Journal of Medical Systems*, vol. 40, no. 4, article no. 96, pp. 1–12, 2019.
- [7]. E. Ahn, L. Bi, Y. H. Jung et al., “Automated saliency-based lesion segmentation in dermoscopic images,” in Proceedings of the 37th Annual International Conference of the *IEEE Engineering in Medicine and Biology Society, EMBC 2015*, pp. 3009–3012, Italy, August 2015.
- [8]. R. B. Oliveira, N. Marranghello, A. S. Pereira, and J. M. R. S. Tavares, “A computational approach for detecting pigmented skin lesions in macroscopic images,” *Expert Systems with Applications*, vol. 61, pp. 53–63, 2016.
- [9]. M. Zortea, E. Flores, and J. Scharcanski, “A simple weighted thresholding method for the segmentation of pigmented skin lesions in macroscopic images,” *Pattern Recognition*, vol. 64, pp. 92–104, 2017.
- [10]. W. Yang, D. Li, S. Wang, S. Lu, and J. Yang, “Saliency-based color image segmentation in foreign fiber detection,” *Mathematical and Computer Modeling*, vol. 58, no. 3-4, pp. 846–852, 2013.
- [11]. E. Ahn, J. Kim, L. Bi et al., “Saliency-Based Lesion Segmentation Via Background Detection in Dermoscopic Images,” *IEEE Journal of Biomedical and Health Informatics*, vol. 21, no. 6, pp. 1685–1693, 2017.
- [12]. A. Borji, M.-M. Cheng, Li, “Salient object detection: a benchmark,” *IEEE Transactions on Image Processing*, vol. 24, no. 12, pp. 5706–5722, 2015.
- [13]. R. Garnavi, M. Aldeen, M. E. Celebi, A. Bhuiyan, C. Dolianitis, and G. Varigos, “Automatic segmentation of dermoscopy images using histogram thresholding on optimal color channels,” *International Journal of Medicine and Medical Sciences*, vol. 1, no. 2, pp. 126–134, 2011.
- [14]. M. Zortea, S. O. Skrøvseth, T. R. Schopf, H. M. Kirchesch, and F. Godtliebsen, “Automatic segmentation of dermoscopic images by iterative classification,” *International Journal of Biomedical Imaging*, vol. 2020, Article ID 972648, 19 pages, 2011.
- [15]. Q. Abbas, M. Sadaf, A. Akram, Prediction of dermoscopy patterns for recognition of both melanocytic and non-Melanocytic skin lesions, *Computers* 5 (3) (2016) 13.
- [16]. Marco Burrioni, Rosamaria Corona, Giordana Dell’Eva, Francesco Sera, Melanoma computer-aided diagnosis reliability and feasibility study, *Clin. Cancer Res.* 10 (6) (2004) 1881–1886.
- [17]. M. Barzegari, H. Ghaninezhad, P. Mansoori, A. Taheri, Z.S. Naraghi, M. Asgari, Computer-aided dermoscopy for diagnosis of melanoma, *BMC Dermatol.* 5(1) (2005) 8.
- [18]. H. Iyatomi, H. Oka, M.E. Celebi, M. Hashimoto, M. Hagiwara, M. Tanaka, K. Ogawa, An improved internet-based melanoma screening system with dermatologist-like tumor area extraction algorithm, *Computer Med. Imaging Graph.* 32 (7) (2008) 566–579.
- [19]. M.E. Celebi, H.A. Kingravi, B. Uddin, H. Iyatomi, Y.A. Aslandogan, W.V. Stoecker, R.H. Moss, A methodological approach to the classification of dermoscopy images, *Computer Med. Imaging Graph.* 31 (6) (2007) 362–373.
- [20]. J.F. Alcon, C. Ciuhu, W. Ten Kate, A. Heinrich, N. Uzunbajakava, G. Krekels, D. Siem, G. De Haan, Automatic imaging system with decision support for inspection of pigmented skin lesions and melanoma diagnosis, *IEEE J. Sel. Top. Signal Process.* 3 (1) (2009) 14–25.
- [21]. Y. Zhou, M. Smith, L. Smith, R. Warr, A new method describing border irregularity of pigmented lesions, *Skin Res. Technol.* 16 (1) (2010) 66–76.
- [22]. R. Garnavi, M. Aldeen, J. Bailey, Computer-aided diagnosis of melanoma using border- and wavelet-based texture analysis, *IEEE Trans. Inf. Technol. Biomed.* 16 (6) (2012) 1239–1252.
- [23]. Q. Abbas, M. Emre Celebi, I.F. Garcia, W. Ahmad, Melanoma recognition framework based on expert definition of ABCD for dermoscopic images, *Skin Res. Technol.* 19 (1) (2013) e93–e102.
- [24]. Q. Abbas, M.E. Celebi, C. Serrano, I. Fondon Garcia, G. Ma, Pattern classification of dermoscopy images: a perceptually uniform model, *Pattern Recognition* 46 (1) (2013) 86–97.
- [25]. L. Yu, H. Chen, Q. Dou, J. Qin, P.A. Heng, Automated melanoma recognition in dermoscopy images via very deep residual networks, *IEEE Trans. Med. Imaging* 36 (4) (2017) 994–1004.

- [26]. R. Kasmi, K. Mokrani, Classification of malignant melanoma and benign skinlesions: implementation of automatic ABCD rule, *IET Image Proc.* 10 (6)(2016) 448–455.
- [27]. S. Khalid, U. Jamil, K. Saleem et al., “Segmentation of skin lesion using Cohen–Daubechies–Feauveaubiorthogonal wavelet,” *SpringerPlus*, vol. 5, no. 1, article no. 1603, 2016.
- [28]. G. Schaefer, M. I. Rajab, M. E. Celebi, and H. Iyatomi, “Colour and contrast enhancement for improved skin lesion segmentation,” *Computerized Medical Imaging and Graphics*, vol. 35, no. 2, pp. 99–104, 2011.
- [29]. F. Xie and A. C. Bovik, “Automatic segmentation of dermoscopy images using self-generating neural networks seeded by genetic algorithm,” *Pattern Recognition*, vol. 46, no. 3, pp. 1012–1019, 2013.
- [30]. D. Meckbach, J. Bauer, A. Pflugfelder et al., “Survival according to BRAF-V600 tumor mutations An analysis of 437 patients with primary melanoma,” *PLoS ONE*, vol. 9, no. 1, Article ID e86194, 2014.
- [31]. Strobl, C., Boulesteix, A. L., and Augustin, T. (2007). Unbiased split selection for classification trees based on the gini index. *Comput. Stat. Data Anal.* 52, 483–501. doi: 10.1016/j.csda.2006.12.030
- [32]. Tripoliti, E. E., Fotiadis, D. I., and Argyropoulou, M. (2007). A supervised method to assist the diagnosis of Alzheimer's disease based on functional magnetic resonance imaging. *Conf. Proc. IEEE Eng. Med. Biol. Soc.* 2007, 3426–3429. doi: 10.1109/IEMBS.2007.4353067
- [33]. Zhang, D., Shen, D., and Alzheimer's Disease Neuroimaging, I. (2012). Predicting future clinical changes of MCI patients using longitudinal and multimodal biomarkers. *PLoS ONE* 7:e33182. doi: 10.1371/journal.pone.0033182
- [34]. Rathore, S., Habes, M., Iftikhar, M. A., Shacklett, A., and Davatzikos, C. (2017). A review on neuroimaging-based classification studies and associated feature extraction methods for Alzheimer's disease and its prodromal stages. *Neuroimage* 155, 530–548. doi: 10.1016/j.neuroimage.2017.03.057